Photoluminescence and First-principle Calculations of the Single Vacancy in Diamond

Kaiyue WANG *, Wenjin ZHANG

School of Materials Science and Engineering, Taiyuan University of Science and Technology, Taiyuan 030024, Shanxi Province, China

crossref http://dx.doi.org/10.5755/j02.ms.24394

Received 11 October 2019; accepted 31 December 2019

The isolated single vacancy is one of the most common defects in diamond, while it is of considerable interest and importance that significantly influences the optical properties of diamond. Although a number of literature publications about the electron structure and density states of single vacancy in diamond from the density functional theory (DFT) calculations, these results are very difficult to be identified from the perspective of experiments. In this paper, the low-temperature photoluminescence (PL) technology was employed to study the emission properties of single vacancy in diamond, and then the photoionization energy, migration energy and vibrionic structure obtained from PL experiments were compared with these obtained from the first-principle calculations. Results showed that the calculation results agreed well with the PL results for the neutral vacancy while differed for the negatively charged vacancy, indicating that for ultrapure diamond, the vacancy mainly existed in form of the neutral rather than the negatively charged.
Keywords: diamond, point defect, photoluminescence.

1. INTRODUCTION

Diamond is transparent to the visible and infrared light due to its wide band gap (~ 5.47 eV), which leads to the application for lens in the scientific equipment, such as IR-detectors and optical windows [1]. The isolated single vacancy is one of the most common defects in diamond, but it is very important that it significantly influences the optical properties of diamond [2]. The vacancy may be grown-in or created by energy-selected irradiation in diamonds, and it can occur in aggregates with concentrations up to 50 ppm, which persists up to 1100 ℃ [3]. Two common charged configurations, neutral and negative (V^0 and V^-), can be detected by infra-red absorption [4] and PL spectra [5]. The corresponding zero phonon lines (ZPLs) are located at 741 nm and 393.5 nm respectively, known as General Radiation One (GR1) centre and Negative Defect One (ND1) centre. The optical center associated with a positive vacancy was also reported in the boron-doped diamond by Charles et al. [6], but it has still not been verified by other technologies.

So far, a number of literature publications about the vacancy related centers in diamond have also been studied from the theory calculations. Alkauskas et al. investigated the electronic and vibronic structure of the nitrogen-vacancy (NV) defect based on the hybrid functions and the results presented a pronounced vibronic mode at 65 meV [7]. The similar work on the negatively charged silicon-vacancy (Si-V) defects was also reported by Elisa et al. [8]. Takayuki et al [9] predicted that the GeV center had the same split-vacancy crystal structure as the SiV center. The electronic structure and magneto-optical properties of titanium-related point defects in diamond was also studied by Kamil et al. through the hybrid density functional theory [10]. Although there are lots of calculations detailed about the electron structure and density states of single vacancy centers in diamond [11, 12], these results are very difficult to be identified from the perspective of experiments. In this paper, the low-temperature PL technology was employed to study the emission properties of single vacancy in diamond, and then the photoionization energy, migration energy and vibrionic structure obtained from PL experiments were compared with these obtained from the first-principle calculations.

2. EXPERIMENTAL METHODS

This work focuses on the ultrapure chemical vapor deposited ultrapure (CVD) diamonds and high pressure high temperature (HPHT) nitrogen doped diamonds, which are provided by De Beers Company. The concentrations of nitrogen are lower than 0.1 ppm and 10 ppm respectively according to microscopic Fourier transform infrared spectroscopy measurement. The irradiation was performed with a Philips EM430 transmission electron microscope (TEM) into which a dog leg had been introduced, enabling the passage of electrons, but blocking ions, thus providing an ion-free electron beam. The irradiated areas were subjected to a uniform intensity of electrons at 300 keV with a dose of 5×10^{19} e·cm^{-2} over a circular region of approximately 60 μm diameter in the top-hat form. The TEM was particularly suitable for the irradiation because the 300 keV was just larger than the displacement threshold of carbon atoms in diamond (≈ 97 keV) [13].

After irradiation the samples were transferred to Renishaw micro-Raman spectrometers fitted with Oxford Instruments Microstat liquid helium-cooled stages. PL examination was mainly performed with an argon-ion laser

* Corresponding author. Tel.: +86-13753184246.
E-mail address: *wangkaiyue8@163.com* (K. Wang)

using an excitation wavelength of 488 nm, although a few experiments were carried out using the 325 nm excitation with a He–Cd laser. PL spectra were obtained at chosen points at equally spaced points in a rectangular (x, y) array covering the irradiated region and its periphery (a "map"). All the PL results were obtained with liquid helium cooling down to the temperatures of around 7 K. The resolution of the optical system was degraded by the cryostats to about 4 μm lateral resolution and 6 μm depth resolution. The annealing was carried out in an argon gas flow for 30 min, from 200 to 950 °C, in steps of 50 °C.

3. CALCULATION METHODS

First-principles calculations were performed in the DFT framework, implemented in the plane-wave based Vienna ab initio Simulation Package VASP. The Perdew-Burke-Ernzerhof functional under the generalized gradient approximation interaction was taken to describe the exchange and correlation interaction. Plane waves with an energy cutoff of 400 eV were used to expand the Kohn-Sham wave functions, which described the interaction between ion and core electrons by the projector augmented wave methods [14 – 16].

To obtain reliable parameters for the calculation, we optimized the primitive diamond bulk firstly. The equilibrium lattice constant of diamond was 3.57 Å under PBE functional. The 2 × 2 × 2 supercell of diamond was built with containing 64 atoms. All atoms could move freely during geometry. For the calculations of energies and electronic properties, 5 × 5 × 5 k-points in the Monkhorst - Pack grids were used.

4. RESULTS AND DISCUSSION

4.1. Ionization energy

The trapped electron at one defect transmits into the conduction band at the sufficient energy of excitation, and that is the ionization of defect. After this process, the change of the energy level within the bandgap results in the conversion of color centers in PL spectra (so-called "photochromic"). The photochromic studies of the defects are very critical for the investigation of the conversion between the defects. In our studies, the PL technology was employed to study many kinds of diamond, but no signals were found to be associated with V^{2-} and V^{2+} defects in these spectra. The excited states of ND1 center located in the conductive band, and hereby the ND1 signal should not be observed in the PL spectra. However in fact, for the very pure colorless diamond, which was irradiated with the electron dose of 5×10^{19} e·cm^{-2}, the strong ND1 signal was observed but unionized even in the such high-energy of 325 nm (3.8 eV) laser excitation as shown in Fig. 1. The results also presented strong GR1 luminescence and lots of interstitial-related ZPLs (500 ~ 600 nm) at 7 K with the 488 nm excitation.

During the calculation, the single vacancy was modeled by removing one C atom from the supercell, and the charged states of vacancy were controlled by changing the total number of electrons in the super cell. This method resulted in an error due to the electrostatic interactions between their charges and images, and thus the Madelung energy was usually taken to correct the error [17].

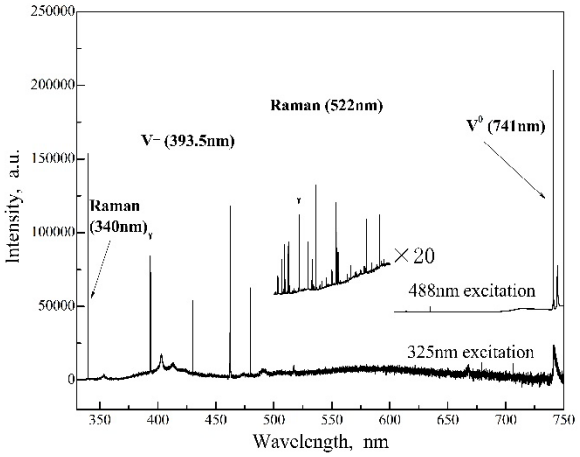

Fig. 1. The typical PL spectra of irradiated ultrapure diamond at ~ 7 K with both 488 nm and 325 nm laser excitation

The formation energy of vacancy E_{vac} with respect to the perfect crystal could be calculated as [18]:

$$E_{vac} = E(q) - E(pure) + \mu + q(\mathrm{E}_{\mathrm{f}}^{0} + E_F), \qquad (1)$$

where *E(q)* is the total energy of the crystal including defect in charge state q; *E(pure)* is the total energy of the perfect crystal, μ_C is the chemical potentials of single C atom in graphite (– 3.518198 eV), $\mathrm{E}_{\mathrm{f}}^{0}$ is the Fermi energy of the neutral vacancy in diamond (11.0938 eV), E_F is the Fermi level with respect to the top of valence band (0 ~ E_g).

The ionizations of charged vacancies could be obtained on basis of the above-mentioned equation. As shown in Fig. 2, the equal formation energy for the 0 and – 1 states at E_F = 0.19 eV was named "ionization level".

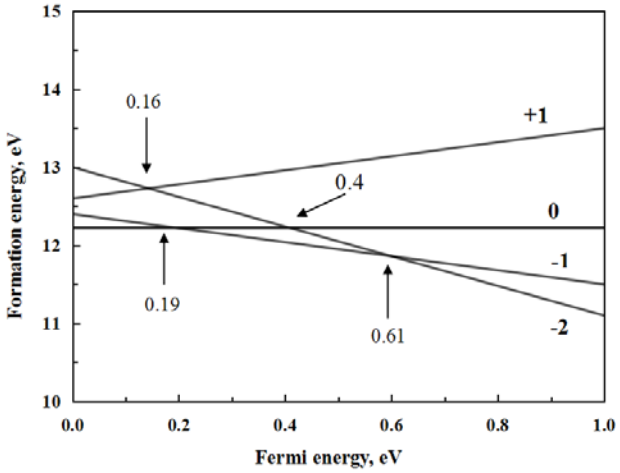

Fig. 2. Formation energies of various charged vacancy in diamond. The Fermi level is referred to the top of valence band

The corresponding ionization levels for (+1, – 2), (0, – 2), (– 1, – 2) were 0.16, 0.4 and 0.61 eV respectively. These results were quite similar to those of R. Long [19]. The (0, – 1) states of the diamond film presented higher ionization level than that of the diamond bulk due to the lower trapping energy of the electron around the vacancy.

In fact, the calculated value of ionization energy for (0, – 1) was obviously larger than that of actual experiment.

4.2. Migration energy

The nitrogen distributions are not uniform in different growth sectors, and Ref. [20] found that the sequence of the nitrogen concentrations, (111) > (311) > (100) > (511) sectors, by compassion of the nitrogen-vacancy (NV) luminescence. Fig. 3 indicated that the GR1 signal decreased while the NV luminescence strengthened with the growing of nitrogen content. In addition, nitrogen atoms acted as the donor provide electrons for the lattice of diamond, which favored the formation of NV- centers. Therefore, the neutral vacancy dominated in the very pure diamond (the nitrogen concentration was less than 0.1 ppm).

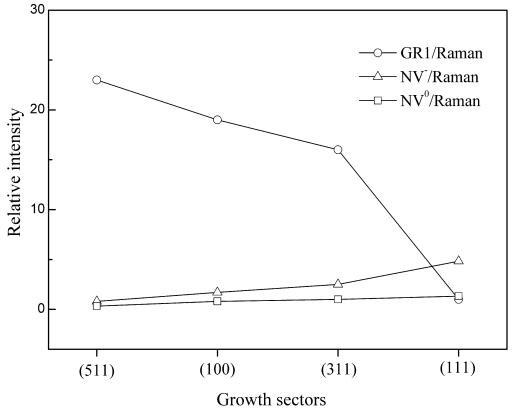

Fig. 3. The relative intensity of some defects in different growth sectors of nitrogen doped diamond

After irradiation with 5×10^{19}e cm^{-2} electrons, lots of single vacancy defects were created in the very pure diamond. The vacancy would move out of the irradiated region in case of such high temperature annealing. The migrating process could be investigated by the PL technology. Fig. 4 presented the variation of the relative intensity of GR1 to Raman in ultrapure diamond during the annealing.

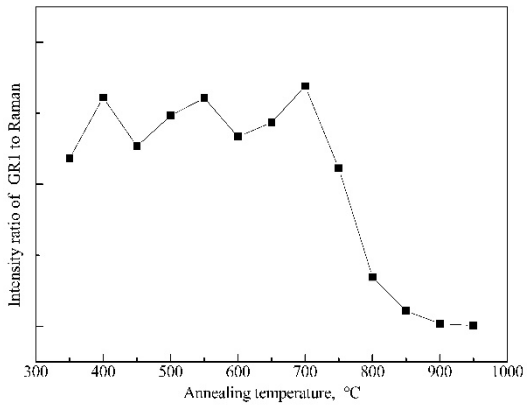

Fig. 4. The relative intensity of GR1 center to Raman in ultrapure diamond during the annealing

It indicated that the vacancy was mobile after 700 ℃, and the corresponding migration energy was 2.9 eV (This value was larger than that of [21]). After 950 ℃ annealing (here we annealed the sample at sufficient high temperature), the intensity “maps” of neutral nitrogen vacancy (NV^0) and GR1 centers on the depth orientation were obtained at 488nm excitation and ~ 7 K (see Fig. 5). The results indicated that the neutral vacancies migrated out of the irradiated region to find nitrogen impurities, and all the nitrogen were converted into NV^0 centers [22].

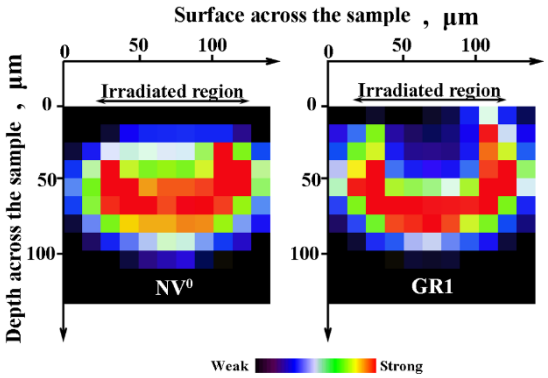

Fig. 5. The intensity distributions of NV^0 and GR1 signals in irradiated ultrapure diamond (the rainbow strength ranged from red to black; the pixels were 25 μm by 25 μm)

The migrating process of the neutral vacancy was also modeled by the first-principle theory. A carbon atom was driven into the neighboring position of neutral single vacancy in diamond. The total energy of the supercell after the geometry varied with the different location of vacancy (see Fig. 6). During geometry, all C atoms could move freely. The results presented that the migrating energy of the single vacancy was 3.1 eV, which was very close to that obtained from our PL results.

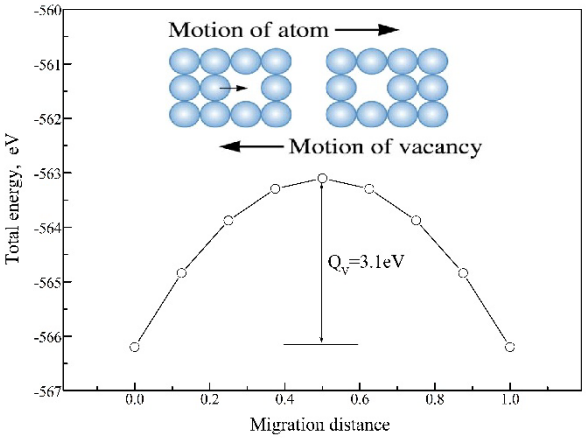

Fig. 6. The total energy of the supercell after the geometry varied with the different location of vacancy

4.3. Vibrionic structure

Fig. 7. Presented the vibronic structures of GR1 and ND1 defects in diamond. Besides the phonon cut-off energy at 165 meV, the strong and wide sidebands were also observed due to the strong electron coupling of the vacancy [23]. Results showed that the vibrations involving only one vacancy were due to two different phonons, one with energy of approximately 42 meV for neutral vacancy and another with approximately 67 meV energy for negative charged. The vibrionic properties of the atoms at the most-neighboring of single vacancy could be also calculated by controlling the states of the atoms in supercell.

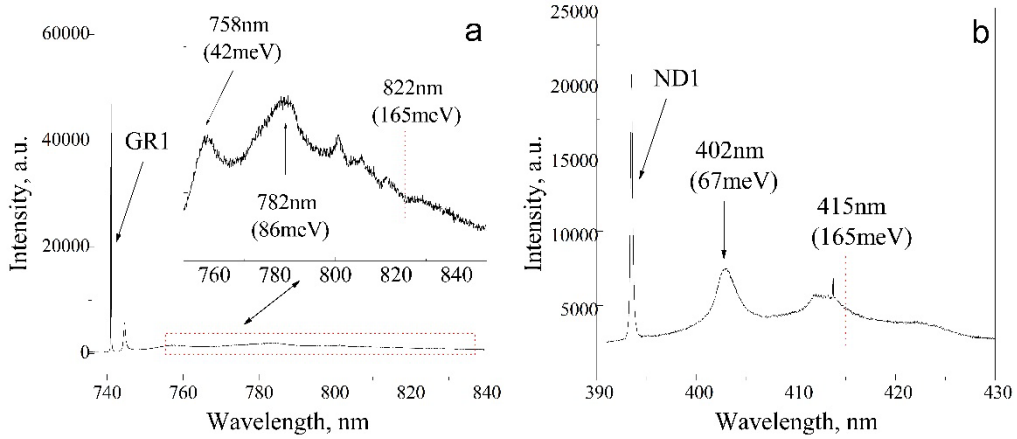

Fig. 7. The vibrionic structures: a – GR1 center in ultrapure diamond obtained with a 488 nm laser at 7 K; b – ND1 center in nitrogen-doped diamond obtained with a 325 nm laser at 7 K

The calculation results indicated that the neutral vacancy involved one phonon with energy of 44.35 meV, which was very close to that of PL experiment. However, the phonon energy for the negative vacancy was calculated as 48.05 meV that was far from that of PL results. The reason could be attributed to the domination of neutral vacancy in ultrapure diamond, which led into the more accurate results for the neutral vacancy.

5. CONCLUSIONS

After electron irradiation, a great number of vacancies and interstitials were created in diamond. The number of vacancies with different charged states mainly depended on the concentration of nitrogen impurity. The higher purity diamond benefited more productions of neutral vacancies. The neutral vacancy had the migration energy of 2.9 eV and phonon energy of 42 meV, which agreed well with these values obtained from the first-principle calculations. However, the corresponding results of negatively charged vacancy were very different between the PL experiments and calculations. The reason was attributed to the domination of neutral vacancy in ultrapure diamond that led into the more accurate results for the neutral vacancy.

Acknowledgments

This work was supported by the Research Project Supported by Shanxi Scholarship Council of China (Grant No. 2020-129), Fund Program for the Scientific Activities of Selected Returned Overseas Professionals in Shanxi Province (Grant No. 20200024) and Shanxi Postgraduate Innovation Project (Grant No 2020SY413, 2020BY107).

REFERENCES

1. **Davis, R.F., Sitar, Z., Williams, B.E., Kong, H.S., Kim, H.J., Palmour, J.W., Edmond, J.A., Ryu, J., Glass, J.T., Carter, Jr.C.H.** Critical Evaluation of the Status of the Areas for Future Research Regarding the Wide Band Gap Semiconductors Diamond, Gallium Nitride and Silicon Carbide *Materials Science and Engineering: B* 1 (1) 1988: pp. 77 – 104. https://doi.org/10.1016/0921-5107(88)90032-3
2. **Saani, H.M., Esfarjani, K., Hashemi, H., Vesaghi, M.A., Basirid, A.R.** Relationship between Lattice Relaxation and Electron Delocalization in Diamond Vacancies *Physica B: Condensed Matter* 376 – 377 2006: pp. 324 – 326. https://doi.org/10.1016/j.physb.2005.12.083
3. **Bangert, U., Barnes, R., Gass, M.H., Bleloch, A.L., Godfrey, I.S.** Vacancy Clusters, Dislocations and Brown Colouration in Diamond *Journal of Physics.Condensed Matter* 21 (36) 2009: pp. 364208. https://doi.org/10.1088/0953-8984/21/36/364208
4. **Yelisseyev, A., Vins, V., Afanasiev, V., Rybak, A.** Effect of Electron Irradiation on Optical Absorption of Impact Diamonds from the Popigai Meteorite Crater *Diamond and Related Materials* 79 2017: pp. 7 – 13. https://doi.org/10.1016/j.diamond.2017.08.012
5. **Kupriyanov, N., Gusev, V.A. Borzdov, Y.M., Kalinin, A.A., Pal'yanov, Y.N.** Photoluminescence Study of Annealed Nickel- and Nitrogen-containing Synthetic Diamond *Diamond and Related Materials* 8 (7) 1999: pp. 1301 – 1309. https://doi.org/10.1016/S0925-9635(99)00122-3
6. **Charles, S.J., Steeds, J.W., Butler, J.E., Evans, D.J.F.** Real and Apparent Grain Sizes in Chemical Vapor Deposited Diamond *Journal of Applied Physics* 57 (22 – 23) 2003: pp. 3090 – 3693. https://doi.org/10.1016/s0167-577x(03)00152-6
7. **Alkauskas, A., Buckley, B.B., Awschalom, D.D., Walle, C.G.V.** First-principles Theory of the Luminescence Lineshape for the Triplet Transition in Diamond NV Centres *New Journal of Physics* 16 2014: pp. 043026. https://doi.org/10.1088/1367-2630/16/7/073026
8. **Londero, E., Thiering, G., Razinkovas, L., Gali, A., Alkauskas, A.** Vibrational Modes of Negatively Charged Silicon-vacancy Centers in Diamond from Ab Initio Calculations *Physical Review B* 98(3) 2018: pp. 035306. https://doi.org/10.1103/PhysRevB.98.035306
9. **Iwasaki, T., Ishibashi, F., Miyamoto, Y., Doi, Y., Kobayashi, S., Miyazaki, T., Tahara, K., Jahnke, K.D., Rogers, L.J., Naydenov, B., Jelezko, F., Yamasaki, S., Nagamachi, S., Inubushi, T., Mizuochi, N., Hatano, M.** Germanium-Vacancy Single Color Centers in Diamond *Scientific Reports* 5 2015: pp. 12882. https://doi.org/10.1038/srep12882
10. **Czelej, K., Ćwieka, K., Śpiewak, P., Kurzydłowskia, K.J.** Titanium-related Color Centers in Diamond: a Density Functional Theory Prediction *Journal of Materials Chemistry C* 19 2018: pp. 5261 – 5268.

https://doi.org/10.1039/C8TC00097B

11. **Breuer, S.J., Briddon, P.R**. Ab Initio Investigation of the Native Defects in Diamond and Self-diffusion *Physical Review B* 51 (11) 1995: pp. 6984 – 6994. https://doi.org/10.1103/PhysRevB.51.6984
12. **Gerstmann, U., Overhof, H.** The New Assignment of Hyperfine Parameters for Deep Defects in Diamond *Physica B: Condensed Matter* 308 – 310 2001: pp. 561 – 564. https://doi.org/10.1016/S0921-4526(01)00733-5
13. **Yuan, D.W., Liu, Z.R.** Atomic Ensemble Effects on Formic Acid Oxidation on PdAu Electrode Studied by First-principles Calculations *Journal of Power Sources* 224 2013: pp. 241 – 249. https://doi.org/10.1016/j.jpowsour.2012.09.113
14. **Kohn, W., Sham, L.J.** Self-consistent Equations Including Exchange and Correlation Effects *Physica Review* 140 (4A) 1965: pp. A1133 – A1138. https://doi.org/10.1103/PhysRev.140.A1133
15. **Clark, S.J., Segall, M.D., Pickard, C.J., Hasnip, P.J., Probert, M.I.J., Refson, K., Payne, M.C.** First Principles Methods Using CASTEP *Zeitschrift fur Kristallographie* 220 (5 – 6) 2005: pp. 567 – 570. https://doi.org/10.1524/zkri.220.5.567.65075
16. **Perdew, J.P., Burke, K., Ernzerhof, M.** Generalized Gradient Approximation Made Simple *Physica Review Letter* 77 (18) 1996: pp. 3865 – 3868. https://doi.org/10.1103/physrevlett.77.3865
17. **Dev, K., Seebauer, E.G.** Vacancy Vharging on Si(1 1 1)-"7×7"Investigated by Density Functional Theory *Surface Science* 572 (2 – 3) 2004: pp. 483 – 489. https://doi.org/10.1016/S0039-6028(03)00734-9
18. **Shim, J., Lee, E.K., Lee, Y.J., Nieminen, R.M.** Density-functional Calculations of Defect Formation Energies Using Supercell Methods: Defects in Diamond *Physica Review B* 71 (3) 2005: pp. 035206. https://doi.org/10.1103/PhysRevB.71.035206
19. **Long, R., Dai, Y., Yu, L., Jin, H., Huang, B.B.** Study of Vacancy on Diamond (100) (2×1) Surface from First-principles *Applied Surface Science* 254 (20) 2008: pp. 6428 – 6482. https://doi.org/10.1016/j.apsusc.2008.04.060
20. **Wang, K.Y., Steeds, J.W., Li, Z.H., Tian, Y.M.** Photoluminescence Studies of Growth-sector Dependence of Nitrogen Distribution in Synthetic Diamond *Materials Characterization* 94 2014: pp. 14 – 18. https://doi.org/10.1016/j.matchar.2014.04.010
21. **Wang, K.Y., Li, Z.H., Tian, Y.M., Zhu, Y.M., Zhao, Y.Y., Chai, Y.S.** Study on Photoluminescence Characteristics of GR1 Center in Diamond *Acta Physica Sinica* 62 (6) 2013: pp. 419-423. https://doi.org/10.7498/aps.62.067802
22. **Davies, G., Campbell, B., Mainwood, A., Newton, M., Watkins, M., Kanda, H., Anthony, T.R.** Interstitials, Vacancies and Impurities in Diamond *Physic and Status Solidi* (a) 186 (2) 2001: pp. 187 – 198. https://doi.org/10.1002/1521-396x(200108)186:2<187::aid-pssa187>3.0.co;2-2
23. **Wang, K.Y., Steeds, J.W., Li, Z.H., Tian, Y.M.** Photoluminescence Studies of Both the Neutral and Negatively Charged Nitrogen-Vacancy Center in Diamond *Microscopy and Microanalysis* 22 (1) 2016: pp. 108 – 112. https://doi.org/10.1017/s1431927615015500
24. **Wang, K.Y., Li, Z.H., Zhang, B., Zhu, Y.M.** Investigation of Vibrionic Structures of Optical Centers in Diamond by Photoluminescence Spectra *Acta Physica Sinica* 61 (12) 2012: pp. 505 – 510.